Journal of Bioenergetics and Biomembranes, Vol. 34, No. 3, June 2002 (© 2002)

EPR Characterization of Ubisemiquinones and Iron–Sulfur Cluster N2, Central Components of the Energy Coupling in the NADH-Ubiquinone Oxidoreductase (Complex I) In Situ

Sergey Magnitsky,[1,2] Larisa Toulokhonova,[1,2,3] Takahiro Yano,[1,2] Vladimir D. Sled,[1,4] Cecilia Hägerhäll,[1,5] Vera G. Grivennikova,[6] Doshimjan S. Burbaev,[7] Andrei D. Vinogradov,[6] and Tomoko Ohnishi[1,8]

Received December 3, 2001; accepted February 12, 2002

The proton-translocating NADH-ubiquinone oxidoreductase (complex I) is the largest and least understood respiratory complex. The intrinsic redox components (FMN and iron–sulfur clusters) reside in the promontory part of the complex. Ubiquinone is the most possible key player in proton-pumping reactions in the membrane part. Here we report the presence of three distinct semiquinone species in complex I in situ, showing widely different spin relaxation profiles. As our first approach, the semiquinone forms were trapped during the steady state NADH-ubiquinone-1 (Q_1) reactions in the tightly coupled, activated bovine heart submitochondrial particles, and were named SQ_{Nf} (fast-relaxing component), SQ_{Ns} (slow-relaxing), and SQ_{Nx} (very slow relaxing). This indicates the presence of at least three different quinone-binding sites in complex I. In the current study, special attention was placed on the SQ_{Nf}, because of its high sensitivities to $\Delta\tilde{\mu}_{H^+}$ and to specific complex I inhibitors (rotenone and piericidin A) in a unique manner. Rotenone inhibits the forward electron transfer reaction more strongly than the reverse reaction, while piericidine A inhibits both reactions with a similar potency. Rotenone quenched the SQ_{Nf} signal at a much lower concentration than that required to quench the slower relaxing components (SQ_{Ns} and SQ_{Nx}). A close correlation was shown between the line shape alteration of the $g_{\|} = 2.05$ signal of the cluster N2 and the quenching of the SQ_{Nf} signal, using two different experimental approaches: (1) changing the $\Delta\tilde{\mu}_{H^+}$ poise by the oligomycin titration which decreases proton leak across the SMP membrane; (2) inhibiting the reverse electron transfer with different concentrations of rotenone. These new experimental results further strengthen our earlier proposal that a direct spin-coupling occurs between SQ_{Nf} and cluster N2. We discuss the implications of these findings in connection with the energy coupling mechanism in complex I.

KEY WORDS: NADH-ubiquinone oxidoreductase; complex I; EPR; ubisemiquinone; iron–sulfur cluster N2; rotenone; piericidin A; energy-transduction.

Key to abbreviations: EPR, electron paramagnetic resonance; SMP, submitochondrial particles; Q, ubiquinone; SQ, ubisemiquinone; Q_1, ubiquinone-1; CCCP, carbonyl cyanide *m*-chlorophenyl hydrazon; RCR, respiratory control ratio; $\Delta\tilde{\mu}_{H^+}$, proton electrochemical gradient; E_m, midpoint redox potential.

[1]Department of Biochemistry and Biophysics, Room 214A, Anatomy–Chemistry Building, Medical School, University of Pennsylvania, 36th and Hamilton Walk, Philadelphia, Pennsylvania 19104-6059.

[2]These authors have equally contributed to this study.

[3]Present address: Hematology Department, The Joseph Stokes Jr. Research Institute, Children Hospital of Philadelphia, Philadelphia, Pennsylvania 19104.

[4]Deceased.

[5]Present address: Department of Biochemistry, Lund University, 22100 Lund, Sweden.

[6]Department of Biochemistry, School of Biology, Moscow State University, Moscow 119 899, Russia.

[7]Institute of Chemical Physics, Russian Academy of Sciences, Moscow 117 977, Russia.

[8]To whom correspondence should be addressed; e-mail: ohnishi@mail.med.upenn.edu.

0145-479X/02/0600-0193/0 © 2002 Plenum Publishing Corporation

INTRODUCTION

NADH-ubiquinone oxidoreductase (complex I) is the electron transfer complex at the entry point of the mitochondrial respiratory chain. Bovine heart complex I consists of 43 subunits and contains one noncovalently bound FMN and at least six EPR-detectable iron–sulfur clusters in situ (Hatefi, 1985; Ohnishi, 1998, Walker, 1992). The complex is composed of two structurally distinct parts: the promontory part, which extrudes into the mitochondrial matrix, and the membrane-spanning part. The former part carries FMN and the iron–sulfur clusters, while the latter is considered to contain ubiquinone-binding sites (Leif *et al*., 1995, Wang *et al.*, 1991; Weiss *et al.*, 1991). The cluster N2 is most likely located in the connection between the promontory and membrane-spanning part. Electrons are transferred from NADH through FMN, iron–sulfur clusters, bound ubiquinone species, and are finally donated to the ubiquinone pool within the lipid phase of the inner mitochondrial membrane. This process of electron transfer drives vectorial proton translocation across the membrane, forming $\Delta\tilde{\mu}_{H^+}$. The consensus value of the experimentally determined proton/2 electron ($H^+/2e^-$) stoichiometry of complex I is 4 (Brown and Brand, 1988; Di Virgilio and Azzone, 1982; Scholes and Hinkle, 1984; Weiss and Friedrich, 1991; Wikström, 1984). Very recently, a $H^+/2e^-$ ratio of 4 has also been estimated based on direct measurement of the initial rates of both H^+ pumping and NADH oxidation in the complex I segment of the respiratory chain in the tightly coupled and activated submitochondrial particles (SMP) (Galkin *et al.*, 1999).

So far little is known experimentally as to the mechanism by which the electron transfer reaction is coupled with the proton-pumping reaction in complex I. Several hypothetical models have been proposed (Brandt, 1997, 1999; Degli Esposti and Ghelli, 1994; Dutton *et al.*, 1998; Krishnamoorthy and Hinkle, 1988; Mitchell, 1966; Ohnishi and Salerno, 1982; Ragan, 1990; Vinogradov, 1993; Weiss and Friedrich, 1991). Recent hypothetical models assume that the energy-coupling reaction operates at the final electron-transfer step between the iron–sulfur cluster N2 and the ubiquinone pool. These models hypothesize that cluster N2 and two or three quinone species function at specific sites within complex I to participate in the site I energy-transducing reaction (Brandt, 1997, 1999; Degli Esposti and Ghelli, 1994; Dutton *et al.*, 1998). The cluster N2 has the highest midpoint redox potential (E_m) among the iron–sulfur clusters in complex I, and its E_m value is pH-dependent (−60 mV/pH) within the physiological pH range (Ingledew and Ohnishi, 1980; Meinhardt *et al.*, 1987; Ohnishi, 1979). The PSST subunit (designated Nqo6/NuoB subunit for the *Paracoccus denitrificans/Escherichia coli* counterpart) has been proposed as the most likely candidate to bear cluster N2 (Ahlers *et al.*, 2000b; Finel *et al.*, 1994; Friedrich, 1998; Leif *et al.*, 1995; Ohnishi, 1998; Yano *et al.*, 1999; Yano and Yagi, 1999).

The EPR properties of ubisemiquinone (SQ) species with different spin-relaxation profiles have been studied in bovine heart SMP during steady state NADH or succinate oxidation (Burbaev *et al.*, 1989; de Jong and Albracht, 1994; Kotlyar *et al.*, 1990; Ohnishi *et al.*, 1998; van Belzen *et al.*, 1997; Vinogradov *et al.*, 1995). Both Vinogradov–Ohnishi's and Albracht–Dunham's groups agreed on the presence of fast-relaxing and uncoupler-sensitive SQ species (de Jong and Albracht, 1994; Ohnishi *et al.*, 1998; van Belzen *et al.*, 1997; Vinogradov *et al.*, 1995) in complex I. Both groups reported the splitting of the $g_{\|} = 2.05$ signal of cluster N2, which was observed only in the tightly coupled SMP. However, there has been a disagreement in interpreting the cause of the splitting. Vinogradov *et al.* have interpreted that the split signal arises from a spin–spin interaction between the fast-relaxing SQ_{Nf} species and cluster N2 (Ohnishi *et al.*, 1998; Vinogradov *et al.*, 1995). Albracht and colleagues have proposed that splitting arises from an exchange–interaction between two "iron–sulfur N2 clusters" that reside in the same subunit (TYKY/Nqo9/NuoI) and have identical intrinsic g factors (van Belzen *et al.*, 1997), although the presence of two "N2 clusters" in the TYKY subunit seems unlikely because of pH-independent E_m values of "these clusters" (Rasmussen *et al.*, 2001).

To attain further insight regarding the functional role of SQ_{Nf} species, we have analyzed the SQ signals arising from complex I in situ, utilizing an NADH-Q_1 reductase system in the tightly coupled, activated bovine heart SMP in the presence of inhibitors for complex II and III. We resolved the complex I-associated SQ signals into three different SQ species without interference from SQ signals arising from complex II and III in the mitochondrial respiratory chain. These new experimental results revealed the presence of a $\Delta\tilde{\mu}_{H^+}$-sensitive fast-relaxing SQ_{Nf} species, as well as the presence of two slow-relaxing $\Delta\tilde{\mu}_{H^+}$-insensitive SQ species in complex I. We also studied the effects of complex I inhibitors on the cluster N2 and SQ signals under various experimental conditions to further demonstrate that spectral changes of cluster N2 and SQ_{Nf} are closely correlated. We will discuss the possible functional role of SQ_{Nf} and cluster N2 in the electron/proton transfer reaction in the complex I segment of the respiratory chain.

MATERIALS AND METHODS

SMP were prepared from bovine hearts obtained at a local slaughterhouse (MOPAC) in Lansdale, PA, and activated by the method previously described (Kotlyar and Vinogradov, 1990). Complex I was deactivated by incubating activated particles in the absence of NADH around 37°C for 30 min according to Kotlyar and Vinogradov (1990). The efficiency of energy coupling in SMP was increased by inhibiting the proton leak with suitable amount of oligomycin according to Grivennikova *et al.* (1997). The degree of activation was determined as follows: (1) The NADH oxidase activity was measured in the presence of 10 mM $MgCl_2$ which inhibits activation (Kotlyar *et al.*, 1992), using 340-nm absorption after preconditioning of SMP with 5 μM NADH, and (2) the NADH oxidase activity was fully activated using the method described above. The ratio of activities between (1) and (2) provides the activation/deactivation ratio. Only SMP preparations with the activation ratio higher than 75% and respiratory control ratios (RCR) greater than 5.0 in the NADH oxidase test were used in the steady state experiments for EPR analysis. Protein concentrations were measured using a biuret reagent (Gornall *et al.*, 1949). The FMN and cytochrome *b* content in our SMP preparations were determined according to the literatures (Faeder and Siegel, 1973; Rieske, 1967), respectively.

For a standard activity assay, SMP (to the final concentration of 50–100 μg/mL) were added to a standard reaction mixture containing 0.25 M sucrose, 50 mM Tris-HCl (pH 8.0), 0.2 mM EDTA, and 1 mg/mL bovine serum albumin. NADH-oxidation was measured at 25°C by following the decrease of optical absorbance at 340 nm using 100 μM NADH. The succinate-driven $\Delta\tilde{\mu}_{H^+}$-dependent NAD^+-reduction (reverse electron transfer) was assayed at 25°C with 10 mM succinate and 1 mM NAD^+ by following the increase in optical absorbance at 340 nm. An extinction coefficient $\Delta\varepsilon_{mM}$ (at 340 nm) = 6.22 mM^{-1} cm^{-1} for NADH was used for calculation. Succinate-oxidase activity was measured with 10 mM succinate in the standard reaction mixture at 25°C by a polarographic method using a Clark-type oxygen electrode. The enzyme activities of "uncoupled" SMP were measured in the presence of 27 μM CCCP. Other additions and details of the experiments are described in their respective figure legends.

Samples for EPR measurements were prepared by placing an SMP suspension in the standard reaction mixture (at a protein concentration of 15–25 mg/mL) into an EPR tube, then adding substrates using a specially designed manual rapid mixing device. The steady state forward electron transfer (NADH $\rightarrow$ O_2 or NADH $\rightarrow$ Q_1) was initiated by adding 1 mM NADH. For the NADH $\rightarrow$ Q_1 reaction, 480 μM Q_1 was premixed as an exogenous electron acceptor together with appropriate amounts of inhibitors for complex II and III. Succinate-supported, $\Delta\tilde{\mu}_{H^+}$-dependent reduction of complex I was started by adding 10 mM succinate. EPR tubes with SMP suspension (treated or not treated with the inhibitors) were preincubated at 25°C for 1 min. Within 3–7 s after adding a substrate, the sample was rapidly frozen in the isopentane/cyclohexane mixture (5:1) at about -140°C and stored in liquid nitrogen until EPR analysis.

To verify that SMP were frozen under an aerobic condition, the EPR signals at $g = 3$ and $g = 6$ of cytochrome *a* and a_3 at 12 K were compared with those of the air-oxidized SMP. If the $g = 3$ signal amplitude decreased more than 20%, we regarded the sample as partially anaerobic and discarded it. The reduction level of the iron–sulfur clusters in complex I during steady state NADH oxidation was compared with that of a fully reduced sample.[9] Ubisemiquinone concentrations were determined by double integration of the experimental spectra recorded at 40 K and microwave power 8 μW in the sample reduced by NADH in the presence of Q_1 and inhibitors for complex II and III. The concentration of cluster N2 and N1b were determined from double integration of simulated whole spectra and from double integration of the half of $g_{\|} = 2.05$ and 2.03 signals recorded under non-power-saturated conditions at 16 and 45 K, respectively (Aasa and Vänngård, 1975; Beinert and Albracht, 1982). A copper standard (0.5 mM Cu(II)-EDTA) was used as a reference. For quantitation of SQ spin concentrations, 500 μM 3-maleimidomethyl-1-proxyl was used as a standard (Miki *et al.*, 1992). In the experiments with complex I inhibitors, the coupled and activated SMP were incubated with different concentrations of inhibitors for at least 20 min on ice prior to the addition of a substrate. Enzymatic activities of all SMP preparations were always checked spectrophotometrically before EPR samples were made. EPR spectra were recorded by a Bruker ESP 300 spectrometer at X-band (9.4 GHz), using an Oxford Instrument ESR-9 helium flow cryostat to control desired sample temperature. Power saturation data were analyzed by computer fitting analysis as described previously (Rupp *et al.*, 1978; Vinogradov *et al.*, 1995).

[9] We refer to a fully reduced sample, which was reduced by NADH under the anaerobic condition.

RESULTS

Previously, we have reported the presence of three distinct SQ species with different spin relaxation properties in the activated, tightly coupled bovine heart SMP during steady state NADH oxidation (abbreviated as NADH $\rightarrow$ O_2 reaction hereafter) (Vinogradov *et al.*, 1995). As shown in Fig. 1(A) at 40 K, a computer analysis of the power saturation curve exhibits a fast-relaxing component SQ_{Nf} ($P_{1/2} = 249$ mW), a slow-relaxing component SQ_{Ns} ($P_{1/2} = 1.57$ mW), and a very slow relaxing component SQ_x ($P_{1/2} = 0.14$ mW). To determine whether these three signals were associated with complex I, we compared SQ signals detected in SMP

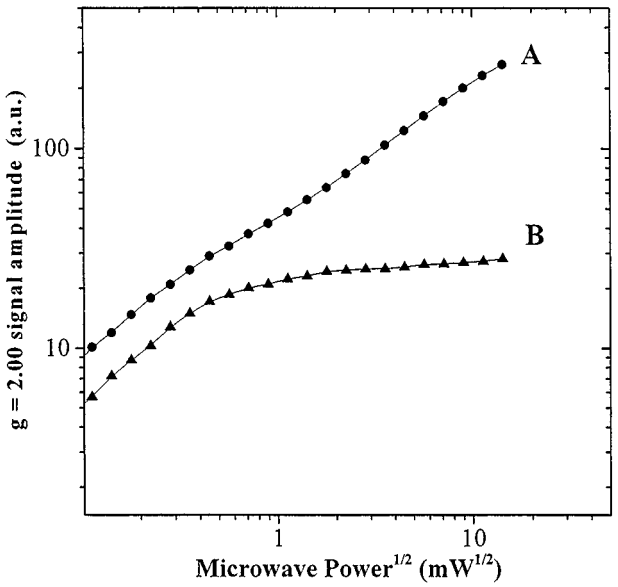

Fig. 1. Progressive power saturation of ubisemiquinone $g = 2.004$ EPR signal recorded at 40 K. (A) Circles—steady state aerobic NADH oxidation reaction (we abbreviate this as NADH $\rightarrow$ O_2 reaction) by tightly coupled, activated SMP (17 mg/mL). The steady state forward electron transfer was initiated by addition of 1 mM NADH. (B) Triangles—steady state succinate $\rightarrow$ O_2 reaction by tightly coupled SMP with deactivated complex I (17 mg/mL). Reaction was initiated by addition of 10 mM succinate. Samples were prepared as described under Materials and Methods. Sample temperature, 40 K; microwave frequency, 9.452 GHz; modulation frequency, 100 kHz; conversion time, 163.8 ms; time constant, 163.8 ms; modulation amplitude, 5 gauss. Best-fit theoretical curves ($A = \sum_{i=1}^{n} C_i \sqrt{P}/(1 + P/P_{1/2(i)})^{0.5 \cdot b_i}$) are drawn through experimental points, corresponding to the sum of individual power saturation curves with following parameters. Curve A: fast-relaxing SQ_{Nf}: $C_1 = 10$, $P_{1/2(1)} = 249$ mW, $b_1 = 0.9$; slow-relaxing SQ_{Ns}: $C_2 = 7$, $P_{1/2(2)} = 1.57$ mW, $b_2 = 0.8$; very slow relaxing SQ_x: $C_3 = 21$, $P_{1/2(3)} = 0.14$ mW, $b_3 = 1$. Curve B: slowly-relaxing SQ_x: $C = 10$, $P_{1/2} = 0.14$ mW, $b = 1$. C = relative concentration, $P_{1/2}$ = half saturation parameter, b = parameter of homogeneity, i = number of components.

containing activated and deactivated complex I. SMP bearing activated complex I were deactivated as described under Materials and Methods. SMP with deactivated complex I shows a pronounced lag phase for NADH oxidation and extremely low reverse electron transfer activity, while the activities of other complexes in the mitochondrial electron transfer chain was not affected by this treatment (Kotlyar *et al.*, 1992; Kotlyar and Vinogradov, 1990). EPR spectra of the deactivated SMP did not show signals of any iron–sulfur clusters of complex I during succinate oxidation, indicating that complex I is completely deactivated (data not shown). Deactivated SMP reduced by succinate had a single, very slow relaxing SQ signal with $P_{1/2}$ (0.14 mW) at 40 K (Fig. 1, curve B). These results indicate that at least two SQ species, SQ_{Nf} and SQ_{Ns}, are associated with complex I.

In SMP, during the aerobic steady state NADH oxidation, we detected SQ signals arising from complex I, II, and III of the mitochondrial respiratory chain. To exclude SQ signals from complex II and III, we used Q_1 as the electron acceptor and measured the NADH $\rightarrow$ Q_1 reductase activity in the presence of inhibitors for complex II and complex III. In bovine heart SMP, NADH $\rightarrow$ Q_1 reductase activity is kinetically comparable to that involving the endogenous Q_{10}, and its reaction is effectively inhibited by rotenone, but is not affected by complex III inhibitors (Lenaz, 1998). The content of cytochrome *b* (b_H and b_L) in our preparation was determined as approximately 0.37 nmol/mg of protein following the method of Rieske (1967). To eliminate the SQ signal from complex III (SQ_i), we added a fivefold excess of complex III inhibitors (antimycin A and myxothiazol). At these inhibitor concentrations, the SQ signal of complex III was completely abolished while its succinate-oxidase activity was inhibited by more than 95% without disturbing the EPR signals from complex I (data not shown). In our SMP preparations during succinate or NADH oxidation, the SQ signal from complex II (SQ_s) was not EPR visible in the temperature range of 16–40 K and at the microwave power level of 1–2 mW. The SQ_s signal was visible at a temperature lower than 10 K and microwave power levels higher than 20 mW. To ascertain that we did not have any interference from the SQ_s signal, we added carboxin at a concentration of 30 nmol/mg of protein. This concentration did not affect the SQ signals of complex I but was high enough to abolish the SQ_s signal completely. Using the NADH $\rightarrow$ Q_1 experimental system in the presence of these complex II and III inhibitors, we detected SQ_{Nf} and SQ_{Ns} signals as well as a signal from a very slow relaxing SQ component. The contribution of this very slow relaxing signal was significantly smaller in the NADH $\rightarrow$ Q_1 experimental system than in the NADH $\rightarrow$ O_2 system

Table I. Contribution of Different SQ Species to the Total Free Radical Signal

	Assay system and relative contribution (%)	
SQ species	NADH → O_2[a,b]	NADH → Q_1[b,c]
SQ_{Nf}	30 ± 5	50 ± 5
SQ_{Ns}	20 ± 5	15 ± 5
$SQ_i + SQ_{Nx}$	50 ± 10	35 ± 10[d]

[a] The total spin concentration of SQ was determined to be 0.17 nmol/mg of protein in the NADH → O_2 system during NADH steady state oxidation.

[b] Spin concentration of iron–sulfur cluster N2 and the FMN content in our SMP are 0.08 nmol/mg and 0.073 nmol/mg, respectively.

[c] The total spin concentration of SQ was determined to be 0.08 nmol/mg of protein in the NADH → Q_1 system during NADH steady state oxidation in the presence of an exogenous electron acceptor Q_1 and inhibitors of complex II and III.

[d] SQ_{Nx} only.

(Table I). On the basis of the experiments with deactivated complex I and the experiments using Q_1, we were able to distinguish two very slow relaxing SQ species. One was antimycin- and myxothiazol-sensitive, and most likely corresponds to SQ_i from complex III. The other SQ was antimycin- and myxothiazol-insensitive, but sensitive to complex I inhibitors (see below). We tentatively attributed the antimycin- and myxothiazol-insensitive, very slow relaxing SQ component to complex I and named it as SQ_{Nx}. The contributions of different SQ species to the total $g = 2.00$ signal in the NADH → O_2 and NADH → Q_1 experimental systems are presented in Table I.

In the present work, we have focused on the analysis of the SQ_{Nf} component of the total SQ free radical signal detected in tightly coupled, activated SMP during NADH → O_2 or NADH → Q_1 steady state reaction. To simplify our further analysis, we have combined SQ_{Ns} and SQ_x (or SQ_{Ns} and SQ_{Nx}) species and treated them as one component, SQ_{slow}. The concentration of SQ_{slow} is equal to the sum of concentrations of the slow- and extremely slow-relaxing components. Since both $P_{1/2}$ values of SQ_{Ns} ($P_{1/2}$ = 1–10 mW) and SQ_{Nx} ($P_{1/2}$ = 0.1–2 mW at 40 K) are much lower than that of the SQ_{Nf} ($P_{1/2}$ = ~200 mW at 40 K), this treatment did not affect the analysis of SQ_{Nf}.

Temperature-Dependence of Complex I-Associated Ubisemiquinone Signals

To further characterize SQ signals associated with complex I, we studied the temperature-dependence of the $g = 2.004$ signal in the NADH → Q_1 system in the presence of inhibitors for complex II and III. Figure 2 depicts individual temperature-dependence of the SQ_{Nf} and SQ_{slow} signals, utilizing coupled and uncoupled SMP, respectively. The SQ_{Nf} signal in the former system was specifically measured at the microwave power of 50 mW. Under this condition, the SQ_{slow} signals were mostly power-saturated, and only SQ_{Nf} signal was detected (curve A). In the latter system only SQ_{slow} signals are detectable, where 0.01 mW was used to assure their nonsaturated condition (curve B). Both data were plotted as a reciprocal function of temperature in the range of 25–55 K. A linear dependence of the signal amplitude of SQ_{slow} signals on reciprocal temperature (curve B) indicates that the SQ_{slow} virtually follows the Curie law; i.e., SQ_{slow} components are magnetically isolated from the environment or their interaction with paramagnetic iron–sulfur cluster(s) is very weak. The SQ_{slow} detectable in SMP treated with different inhibitors also follows the Curie law, as in the case of curve B. Curve A, in contrast, shows strong deviation of the temperature-dependence of the SQ_{Nf} species from the Curie law which indicates that, unlike the SQ_{slow}, this SQ_{Nf} species interacts magnetically with a nearby paramagnetic center(s).

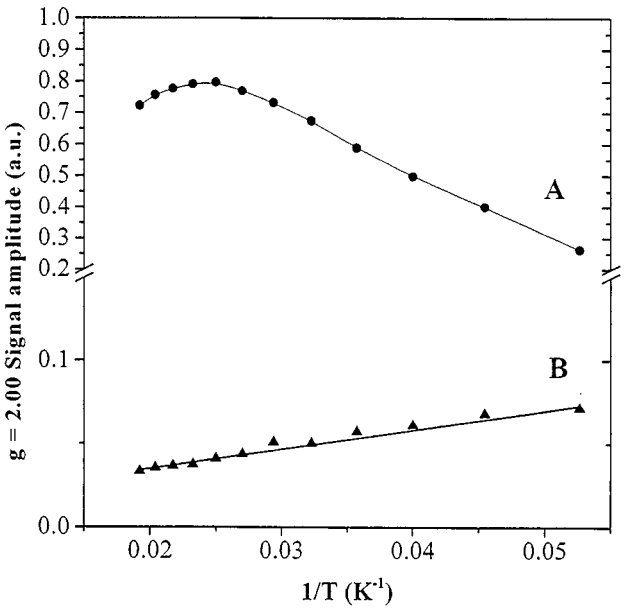

Fig. 2. Temperature-dependence of ubisemiquinone signals. (A) Circles—NADH → Q_1 steady state reaction. The reaction mixture contained 21 mg/mL of SMP, 1 mM NADH, 480 μM Q_1, 1.25 nmol/mg each of antimycin A and myxothiazol, and 30 nmol/mg carboxin. (B) Triangles—the same as (A), except 27 μM CCCP was added. EPR conditions: microwave power levels 50 mW (A) and 0.01 mW (B). Other EPR conditions were same as in the Fig. 1 legend.

$\Delta\tilde{\mu}_{H^+}$-Dependence of Complex I-Associated Ubisemiquinones

To examine the effects of electrochemical proton gradient on SQ signals of complex I, we analyzed spin relaxation properties of the semiquinones in the coupled and uncoupled SMP. Figure 3 shows power saturation curves of SQ signals in the coupled (curve A) and uncoupled (curve B) SMP during the steady state NADH-Q_1 oxidoreduction at 40 K. Computer analysis of these two curves revealed the presence of the SQ_{Nf} component in the coupled SMP, whereas this was absent in the uncoupled SMP. Computer simulation of the power saturation curves showed that an approximately equal quantity of the SQ_{Ns} and SQ_{Nx} components were present in both samples, showing that both slow-relaxing SQ species are $\Delta\tilde{\mu}_{H^+}$-independent. To further analyze the effects of $\Delta\tilde{\mu}_{H^+}$ poised across the membrane on the SQ signal amplitude, we prepared SMP in the presence of different concentrations of oligomycin, which increases the RCR by inhibiting proton leaks in ATPsynthase (Lee and Ernster, 1967). We analyzed power saturation profiles of the SQ signals in SMP with different RCR during the steady state NADH $\rightarrow$ O_2 reaction. Table II shows the contribution of the SQ_{Nf} to the total SQ signals detected in the SMP samples with different RCR. The total SQ spin content increased as the oligomycin concentration increased. When SMP was completely uncoupled, we could not detect the SQ_{Nf} component (Fig. 3). When RCR is 1.5, the contribution of the SQ_{Nf} signal is only 5.5%, and in tightly coupled SMP with RCR = 9, the contribution of the SQ_{Nf} signal reached its maximum of 30% of the total SQ free radical signal. These results demonstrate that the SQ_{Nf} signal is very sensitive to $\Delta\tilde{\mu}_{H^+}$ whereas the SQ_{slow} components are not.

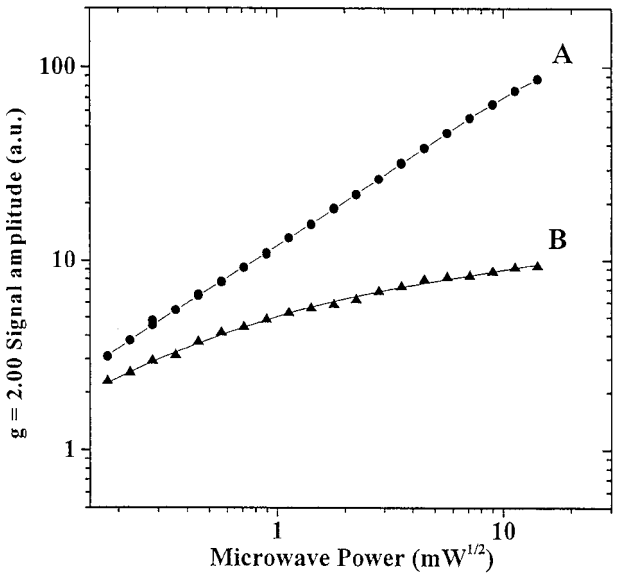

Fig. 3. Progressive power saturation of ubisemiquinone $g = 2.00$ EPR signal in coupled (A) and uncoupled (B) bovine heart SMP recorded at 40 K. (A) Circles—the NADH $\rightarrow$ Q_1 steady state reaction by the tightly coupled SMP (21 mg/mL) in the presence of 1 mM NADH, 480 μM Q_1, 1.25 nmol/mg each of antimycin A and myxothiazol, and 30 nmol/mg carboxin. (B) Triangles—the same as (A) except that 27 μM CCCP was added. Parameters of theoretical curves (see Fig. 1): Curve A (coupled SMP): fast-relaxing SQ_{Nf}: $C_1 = 7$, $P_{1/2(1)} = 220$ mW, $b_1 = 0.85$; slow-relaxing SQ_{Ns}: $C_2 = 2.2$, $P_{1/2(2)} = 1.4$ mW, $b_2 = 0.8$; very slow relaxing SQ_{Nx}: $C_3 = 5.7$, $P_{1/2(3)} = 0.08$ mW, $b_3 = 0.9$. Curve B (uncoupled SMP): fast-relaxing SQ_{Nf}: $C_1 = 0.001$, $P_{1/2(1)} = 220$ mW, $b_1 = 0.82$; slow-relaxing SQ_{Ns}: $C_2 = 2.05$, $P_{1/2(2)} = 1.4$ mW, $b_2 = 0.8$; very slow relaxing SQ_{Nx}: $C_3 = 5.5$, $P_{1/2(3)} = 0.08$ mW, $b_3 = 0.9$.

Table II. RCR-Dependence of the Fast-Relaxing Ubisemiquinone (SQ_{Nf}) in the NADH $\rightarrow$ O_2 System

Oligomycin (nmol/mg of protein)	RCR	Contribution of fast-relaxing ubisemiquinone (SQ_{Nf}) (%)[a]
0	1.5	5.5 ± 3
0.125	2.7	6.6 ± 4
0.21	5.5	15 ± 5
0.42	9.0	30 ± 5

[a] Total SQ spin concentrations detected in SMP with RCR of 2.7 and 9.0 were 0.06 nmol/mg and 0.10 nmol/mg, respectively.

Effects of Specific Inhibitors of Complex I on the Fast-Relaxing Component SQ_{Nf}

To further investigate the properties of SQ_{Nf}, we performed experiments, using two specific inhibitors of complex I, namely, rotenone and piericidin A. The NADH oxidase activity of our SMP preparations was effectively inhibited by rotenone and piericidin A with I_{50} values of 0.045 nmol/mg and 0.035 nmol/mg, respectively, in the standard assay conditions (see Materials and Methods). We analyzed the effects of these two inhibitors on EPR signals of SQ_{Nf} and SQ_{slow}, which were individually monitored at two different microwave power levels, 126 and 0.02 mW, respectively. Figure 4(A) shows the quenching of the SQ_{Nf} and the SQ_{slow} signals by different concentrations of piericidin A (recorded at 40 K). It is clearly seen that the SQ_{Nf} and the SQ_{slow} components decreased almost in parallel as the inhibitor concentration increased. The I_{50} values for the SQ_{Nf} and the SQ_{slow} are about the same, each 0.024 (nmol/mg of protein). In contrast, the effects of rotenone on the two distinct SQ species are different (Fig. 5(A)). The SQ_{Nf} component revealed a higher sensitivity to rotenone than did the SQ_{slow} component. The I_{50} values for the SQ_{Nf} and the SQ_{slow} were

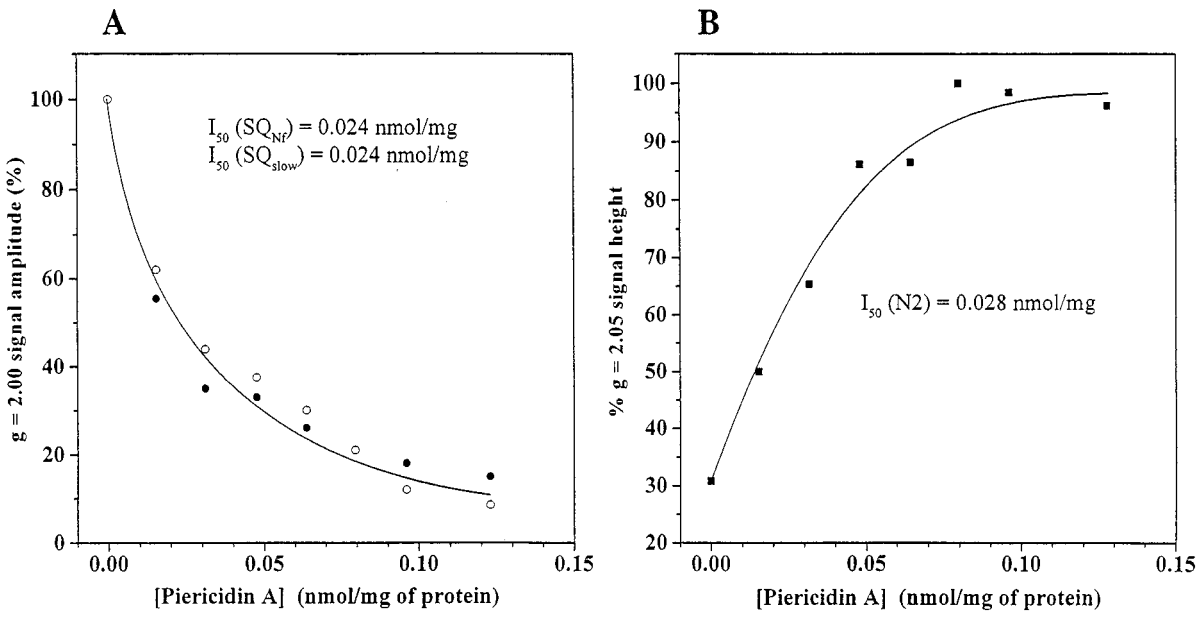

Fig. 4. (A) Effects of piericidin A on the $g = 2.00$ signal amplitude at two different power levels in the NADH $\rightarrow O_2$ reaction by the tightly coupled SMP (18 mg/mL). Open circles—microwave power, 126 mW; closed cycles—microwave power, 0.02 mW. The reaction was initiated by the addition of 1 mM NADH. The samples were prepared as described under Materials and Methods. We defined I_{50} (N2) as a concentration of inhibitors at which the amplitude (A) of $g_{\|} = 2.05$ equals a half of the sum of the N2 signal amplitude in the fully reduced (fr) sample and in the samples under NADH steady state (st-s) oxidation: I_{50} (N2) $= {}^1/_2[A(\text{N2})_{\text{st-s}} + A(\text{N2})_{\text{fr}}]$. From Figure 4(A) we obtained I_{50} (SQ_{Nf}) = 0.024 nmol/mg of protein and I_{50} (SQ_{slow}) = 0.024 nmol/mg of protein. EPR conditions: microwave frequency, 9.452 MHz; modulation frequency, 100 kHz; conversion time, 163.8 ms; time constant, 163.8 ms; modulation amplitude, 5 gauss; sample temperature, 40 K. (B) Dependence of the $g_{\|} = 2.05$ peak height of iron–sulfur cluster N2 on piericidin A concentrations in the NADH $\rightarrow O_2$ reaction by the tightly coupled SMP (18 mg/mL). The I_{50} (N2) was determined to be 0.028 nmol/mg of protein. EPR conditions: sample temperature, 16 K; microwave power, 1 mW; microwave frequency, 9.452 MHz; modulation frequency, 100 kHz; conversion time, 163.8 ms; time constant, 163.8 ms; modulation amplitude, 5 gauss.

0.055 (nmol/mg of protein) and 0.26 (nmol/mg of protein), respectively. We also determined the contributions of the SQ_{Nf} and SQ_{slow} components to the total SQ signals observed at various inhibitor concentrations by computer curve fitting analyses of the power saturation profiles. The analyses gave consistent results as those presented in Figs. 4 and 5 (data not shown).[10]

Analysis of the $g_{\|} = 2.05$ Signal Behavior Under Different Experimental Conditions

Changes in the $g_{\|}$ line shape of iron–sulfur cluster N2 under different experimental conditions was reported earlier (van Belzen *et al.*, 1997; Vinogradov *et al.*, 1995). Albracht's group reported the appearance of two additional peaks around the $g_{\|} = 2.05$ component of cluster N2 during the steady state oxidation of NADH or succinate (de Jong *et al.*, 1994; de Jong and Albracht, 1994). In experiments with different inhibitors and with coupled and uncoupled SMP, we also observed the change in the line shape of EPR signal at the $g_{\|} = 2.05$ region. We examined the line shape of $g_{\|} = 2.05$ signal in SMP with different RCR. The line shape of the $g_{\|}$ signal in completely uncoupled SMP was almost identical to the signal in the fully reduced anaerobic samples. As RCR increased by the addition of higher concentrations of oligomycin to tightly coupled samples, the $g_{\|} = 2.05$ signal became broadened, or partly split into two peaks at $g = 2.064$ and 2.044, with concomitant decrease of the $g = 2.05$ peak height. As mentioned earlier, the relative contribution of the SQ_{Nf} radical signal also increased with the enhanced RCR. These results indicate that the signal line shape of cluster N2 is also affected by $\Delta\tilde{\mu}_{H^+}$.

[10] It should be noted that the direct comparison between quantitative titrations of the EPR-detectable components by these inhibitors and those of catalytic activities is difficult if not impossible, because of the significant protein concentration difference used in the two experiments. The conditions for distribution of highly hydrophobic inhibitors between aqueous and lipid phases in different experimental approaches are very different.

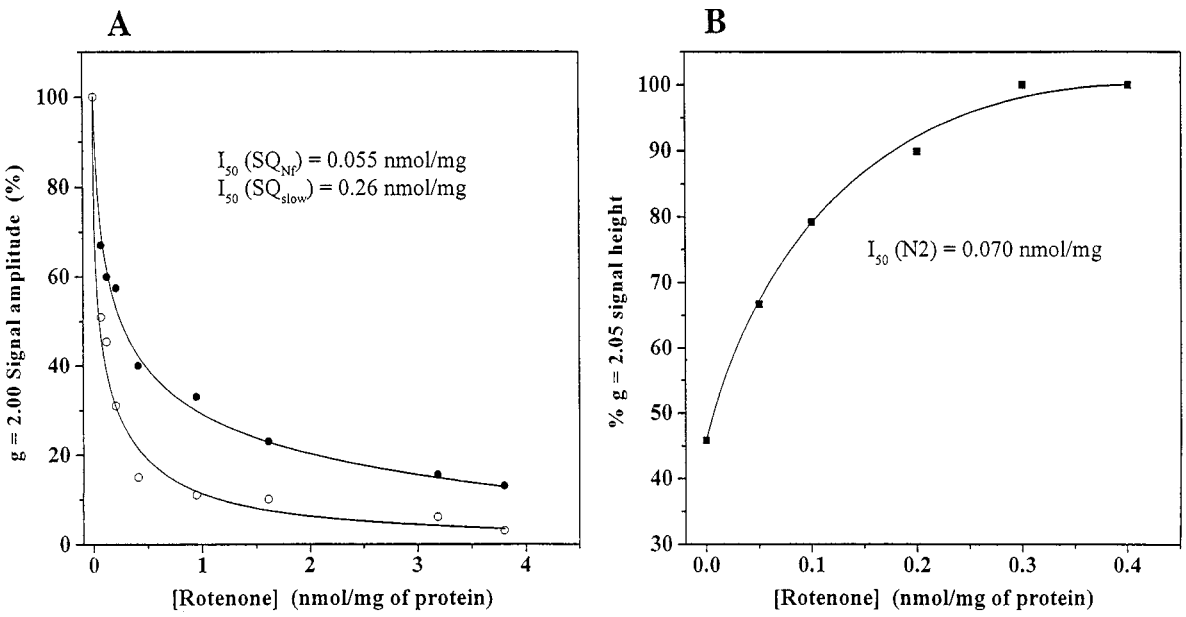

Fig. 5. (A) Effects of rotenone on the $g = 2.00$ signal amplitude at two different power levels in the NADH $\rightarrow O_2$ reaction by the tightly coupled SMP (20 mg/mL). Open circle—microwave power, 126 mW; closed cycles—microwave power, 0.02 mW. The reaction was initiated by addition of 1 mM NADH. We obtained $I_{50}(SQ_{Nf}) = 0.055$ nmol/mg of protein and $I_{50}(SQ_{slow}) = 0.26$ nmol/mg of protein. The samples were prepared as described under Materials and Methods. EPR conditions are same as in Fig. 4(A). (B) Dependence of the $g_{\|} = 2.05$ peak height of iron–sulfur cluster N2 on rotenone concentrations in the NADH $\rightarrow O_2$ reaction by the tightly coupled SMP (20 mg/mL). I_{50} (N2) was determined to be 0.070 nmol/mg of protein. EPR conditions are the same as in Fig. 4(B).

However, we did not observe clear split peaks of the $g_{\|} = 2.05$ signal with most of SMP preparations during the aerobic NADH steady state oxidation reaction. More frequently we observed its broadening; the width of the $g_{\|} = 2.05$ signal at the half peak height became ($\Delta H \sim 11$–12 gauss) compared to that of the fully reduced sample ($\Delta H \sim 9$–10 gauss). The broadening of the line width is much harder to measure accurately than the splitting. Thus in this case, we expressed it as the decrease of the $g_{\|} = 2.05$ peak height. Optimization of EPR conditions for the line shape change of cluster N2 revealed that the temperature and microwave power ranges to observe clear split signals are relatively narrow. In the forward reaction the split signals were seen in the 14–18 K temperature range and at 1–5 mW microwave power levels. In contrast, in the $\Delta\tilde{\mu}_{H^+}$-dependent electron reverse reaction the split signals were seen more clearly at a higher temperature range (16–22 K) and a higher microwave power level (2–20 mW). Figure 6 depicts EPR spectra of the $g_{\|} = 2.05$ region in the steady state succinate $\rightarrow O_2$ (A) and NADH $\rightarrow O_2$ oxidoreduction (B), and in the fully reduced state by NADH in the presence of CCCP (C). The addition of an uncoupler into the reaction mixture led to an increase of the peak amplitude of the $g_{\|} = 2.05$ signal, approaching to that of the fully reduced uncoupled sample. As seen in Figs. 6(A) and 6(B), the split signals were seen, in general, more clearly in succinate-reduced samples in comparison with NADH-reduced samples. We determined spin concentrations of N2 and N1b in our SMP preparations by two different methods as described under Materials and methods. Both methods gave a consistent value of 0.08 nmol/mg for clusters N2 and N1b, which is in reasonable agreement with the FMN content (0.073 nmol/mg) of the same sample.

Temperature-dependence of the signal suggests that the SQ_{Nf} species interacts with a nearby paramagnetic center, which was deduced to be cluster N2 (Burbaev *et al.*, 1989; Vinogradov *et al.*, 1995). Since rotenone and piericidin A inhibit the electron transfer step from N2 to the ubiquinone pool, it was of interest to study the effects of these inhibitors on the EPR properties of cluster N2 itself. The addition of rotenone or piericidin A diminished the splitting of EPR signals causing an increase of the $g_{\|} = 2.05$ peak amplitude, and concomitant quenching of the SQ free radical signals (Figs. 4(B) and 5(B)). The I_{50} for piericidin A obtained for the SQ_{Nf}, SQ_{slow}, and cluster N2 are very close to each other (Fig. 4). It is interesting to note that the situation is different in the case of rotenone, which was shown to have a kinetically different inhibition pattern from piericidin A (Degli Esposti, 1998; Friedrich

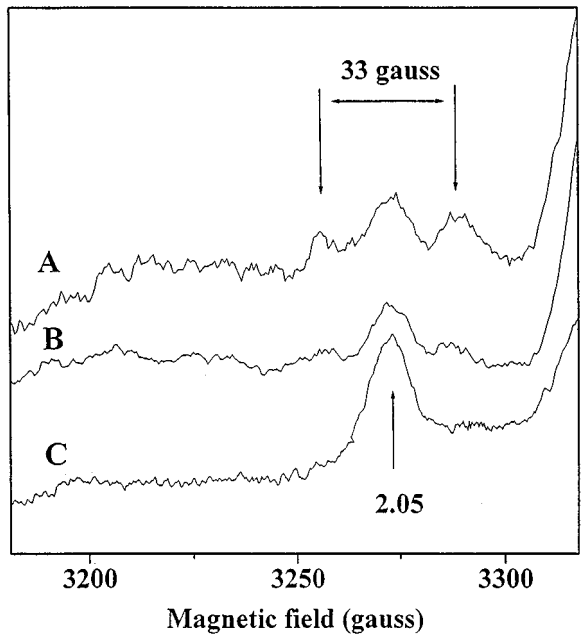

Fig. 6. EPR spectra of the $g_{\|} = 2.05$ region of bovine heart SMP. (A) A spectrum of the tightly coupled and activated SMP (25 mg/mL) during the steady state succinate oxidation recorded at 18 K and 10 mW. (B) A spectrum of tightly coupled SMP (25 mg/mL) during steady state NADH oxidation recorded at 14 K and 1 mW. (C) A spectrum of SMP (25 mg/mL) fully reduced by NADH in the presence of 27 μM CCCP recorded at 16 K and 1 mW. EPR conditions: conversion time, 81.9 ms; time constant, 163.8 ms; microwave frequency, 9.452 MHz; modulation frequency, 100 kHz; modulation amplitude, 5 gauss.

et al., 1994). The I_{50} for the SQ_{Nf} and cluster N2 were almost the same, whereas the I_{50} for the SQ_{slow} species was approximately five times larger than those for the SQ_{Nf} and cluster N2 (Fig. 5).

Examination of the Effects of $\Delta\tilde{\mu}_{H^+}$ on the $g_{\|} = 2.05$ Signal of the Cluster N2

It has been reported that rotenone exhibits significantly different potency for the forward electron transfer activity (NADH oxidase) and for the reversed electron transfer, namely, succinate-driven $\Delta\tilde{\mu}_{H^+}$-dependent NAD^+ reduction (Grivennikova *et al.*, 1997). This provided an additional diagnostic tool system to test "the two N2 cluster" hypothesis (van Belzen *et al.*, 1997). We analyzed the effects of rotenone on the SQ_{Nf} signal and on the signal amplitude of the $g_{\|} = 2.05$ during the steady state succinate oxidation. The addition of 0.083 nmol/mg (corresponds to the 2 μM in the Fig. 7(B)) of rotenone inhibited the NADH oxidase activity to 33%, whereas it affected the reverse reaction only to 73% (Fig. 7(B)). At this concentration of rotenone, we still observed a full reduction of cluster N2 in the tightly coupled, activated SMP during the steady state succinate oxidation. As shown in Fig. 7(A) (i), the $g_{\|} = 2.05$ signal of cluster N2 was considerably broadened in the absence of rotenone. This sample exhibited the SQ_{Nf} signal, which accounted for approximately 24.7% of the total SQ signals. The addition of 0.083 nmol/mg of rotenone not only quenched the SQ_{Nf} signal to 4% as it did for the steady state NADH oxidation, but also caused concomitant sharpening of $g_{\|} = 2.05$ signal, which was almost identical to that of the fully reduced sample (Figs. 7(A) (ii) and (iii)). Since the $\Delta\tilde{\mu}_{H^+}$ formation was maintained by a continuous flow of electrons from succinate through the respiratory chain under these conditions, the loss of the broadening effects on the $g_{\|} = 2.05$ signal can be attributed simply to the quenching of the SQ_{Nf} species. The results shown in Fig. 7 indicate that the line shape change of the $g_{\|} = 2.05$ signal is not caused by $\Delta\tilde{\mu}_{H^+}$ itself.

Resolved EPR Spectrum of the Fast-Relaxing Ubisemiquinone SQ_{Nf}

The use of NADH $\rightarrow Q_1$ experimental system in the presence of inhibitors of complex II and III made it possible to analyze the SQ signals associated only with complex I. The high $P_{1/2}$ value of the SQ_{Nf} species and its extremely high sensitivity to uncoupler allowed us to resolve SQ_{Nf} spectrum from the total $g = 2.00$ signal. Figure 8 shows a difference spectrum, coupled SMP–uncoupled SMP, at 40 K and 20 mW, which represents the spectrum of the SQ_{Nf} signal alone. The g value of the SQ_{Nf} signal is 2.004 in X-band EPR and its peak-to-peak line width is ~8.4 gauss. In a D_2O buffer, the spectral line shape did not significantly change (Yano and Ohnishi, unpublished data). This narrow line width of the signal indicates that the SQ_{Nf} species is mostly anionic ($Q^{\cdot -}$) at pH 8 (Bowyer and Ohnishi, 1985).

DISCUSSION

The energy coupling mechanism in complex I is one of the very important, yet unsolved problems in bioenergetics. Several hypothetical models have been proposed during the last few years (Brandt, 1997,1999; Degli Esposti and Ghelli, 1994; Dutton *et al.*, 1998; Vinogradov, 1993). In these models, at least two bound forms of semiquinone molecules have been postulated to be involved in the proton-pumping reaction linked to the electron transfer from the iron–sulfur cluster N2 (the highest E_m component among complex I iron–sulfur clusters) to the ubiquinone pool. In the present work, we investigated the properties of complex I associated SQ signals detected

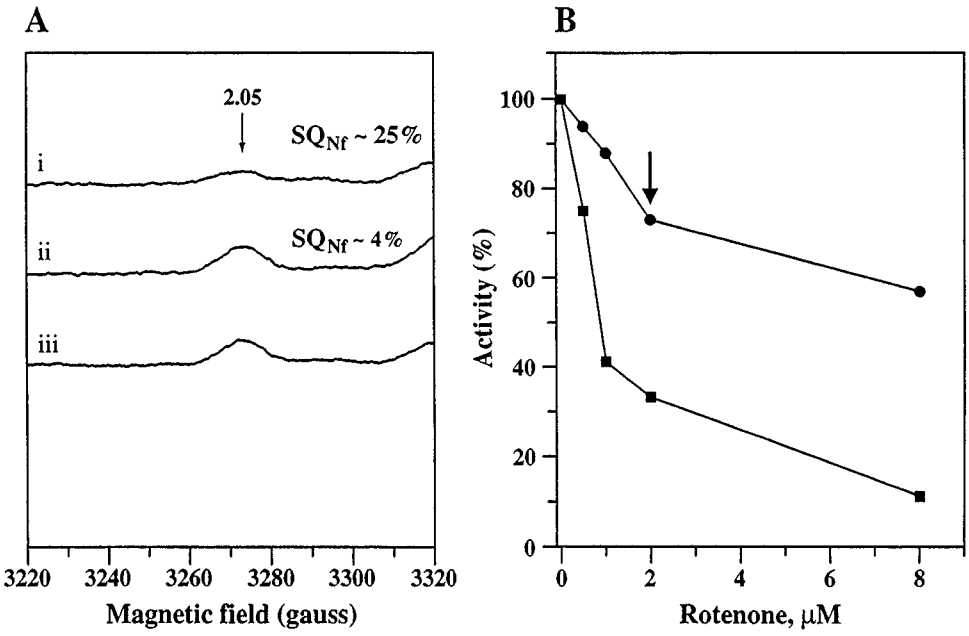

Fig. 7. Effect of rotenone on (A) EPR spectra of the $g_{\|} = 2.05$ region and (B) the forward and reverse electron transfer activities of bovine heart SMP (24 mg/mL). (A) (i) A spectrum of the tightly coupled and activated SMP during the steady state succinate oxidation recorded at 16 K and 5 mW. (ii) A spectrum of the tightly coupled and activated SMP during the steady state succinate oxidation in the presence of 0.083 nmol/mg of rotenone recorded at 16 K and 5 mW. (iii) A spectrum of SMP fully reduced by NADH recorded at 16 K and 1 mW. EPR conditions: conversion time, 81.9 ms; time constant, 163.8 ms; microwave frequency, 9.452 MHz; modulation frequency, 100 kHz; modulation amplitude, 5 gauss. (B) Inhibition of the NADH oxidase activity (NADH $\rightarrow$ O_2) (Filled square) and of the succinate-driven $\Delta\tilde{\mu}_{H^+}$-dependent NAD^+-reduction (reverse electron transfer succinate $\rightarrow$ NAD^+) (filled circle), as a function of varying rotenone concentration.

in the activated, tightly coupled bovine heart SMP during the steady state oxidation of NADH or succinate. We also studied properties of the iron–sulfur cluster N2 under several different conditions and extended the analysis of spin–spin interaction between cluster N2 and SQ by measuring the enhanced spin relaxation of the SQ_{Nf}.

The use of an NADH $\rightarrow$ Q_1 experimental system together with complex II and III inhibitors allowed us to analyze the SQ signals arising only from complex I. We confirmed the presence of the fast-relaxing SQ_{Nf} and the slow-relaxing SQ_{Ns} species in the complex I residing in the inner membrane of bovine heart SMP. Furthermore, we revealed the presence of a very slow-relaxing component SQ_{Nx} associated also with complex I. The steady state equilibrium concentrations of these three complex I-associated SQ species were found to be SQ_{Nf}:SQ_{Ns}:SQ_{Nx} = 0.50:0.15:0.35 relative to one complex I molecule[11] during the NADH-Q_1 oxidoreductase reaction in the tightly coupled SMP. The SQ_{Nf} species has a number of unique properties: (i) The spin relaxation of the SQ_{Nf} signal is extremely fast, for example, with $P_{1/2}$ value of >200 mW at 40 K. (ii) The temperature-dependence of the SQ_{Nf} signal is strongly deviated from the Curie law. (iii) SQ_{Nf} is extremely sensitive to $\Delta\tilde{\mu}_{H^+}$ poised across the mitochondrial inner membrane.

Moreover, the relative intensity of the SQ_{Nf} signal correlates directly with $\Delta\tilde{\mu}_{H^+}$ across the inner membrane of SMP. The addition of uncoupler (CCCP) completely eliminated the SQ_{Nf} signal. An increase of RCR by the addition of oligomycin progressively increased the signal amplitude of SQ_{Nf} species, within an appropriate oligomycin concentration range. The high sensitivity of the SQ_{Nf} species to the poised $\Delta\tilde{\mu}_{H^+}$ suggests that this semiquinone species is directly involved in the proton translocation process in complex I. The SQ_{slow} (SQ_{Ns} and SQ_{Nx}) signals follow the Curie law, and thus these

[11] A contribution of a stable SQ_1 free radical signal to the total SQ signal cannot be completely excluded. A possibility of the presence of artificial signal from exogenous electron acceptors is currently under investigation with different quinone analogs. It should be noted, however, that in the presence of a higher concentration of rotenone (1.5 nmol/mg), we detected only a small fraction of SQ signal (<5% of the SQ signal in the absence of rotenone).

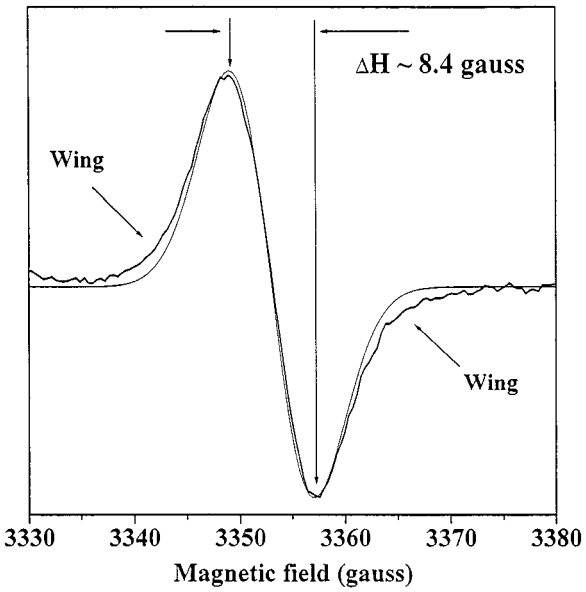

Fig. 8. Resolved ubisemiquinone free radical signals of the SQ_{Nf} and their computer simulation. (A) Solid line—EPR spectrum of the SQ_{Nf} signal as a difference spectrum (coupled SMP–uncoupled SMP) during steady state NADH oxidation in the presence of 480 μM Q_1 and inhibitors of complex II and III at 40 K and microwave power level of 20 mW. Dashed line (—) simulated spectrum with a peak-to-peak line width of 8.4 gauss. EPR conditions are the same as in Fig. 6.

species seem to be located away (>30 Å) from the fast-relaxing paramagnetic center, cluster N2 (Ohnishi *et al.*, 1998; Vinogradov *et al.*, 1995).

To further study SQ signals in complex I, we employed two specific complex I inhibitors, rotenone and piericidin A, which interrupt the electron transfer step between cluster N2 and the ubiquinone pool. Piericidin A quenched SQ_{Nf} and SQ_{slow} signals in the same manner during the forward and reverse electron transfer reactions, whereas rotenone exhibited a more specific inhibitory effect on the SQ_{Nf} signal in comparison with that on the SQ_{slow} signal. To our knowledge, this is the first demonstration that complex I inhibitors (kinetically distinguished class I/II or class A/B) (Degli Esposti, 1998; Friedrich *et al.*, 1994) affect the complex I-associated SQ species in different manners. This finding may provide a new insight into the inhibition mechanism by structurally diverse complex I inhibitors, especially in the light of recently proposed views that these inhibitors share a rather large pocket with partially overlapping binding sites (Okun *et al.*, 1999; Schuler *et al.*, 1999). The significantly different effects of piericidin A and rotenone on the individual semiquinone species as reported in this paper, strongly suggest that three distinct inhibitor binding sites exist.

We found a close correlation between the changes in the $g_{\|} = 2.05$ peak amplitude and the quenching of the SQ_{Nf} signal by these complex I inhibitors. As described earlier in the Results section, we have observed more frequently the spectral broadening (detected as an decrease in the central peak amplitude) than the splitting of the $g_{\|} = 2.05$ signal in $\Delta\tilde{\mu}_{H^+}$ poised SMP preparations (Cammack *et al.*, 1994; Leigh, 1970). At present, the reason for this batch-dependent variation is not fully understood, although one of the reasons seems to be the variation of the RCR ratios (Table II).

The split of $g_{\|} = 2.05$ signal was more frequently observed in the sample where N2 reduction and SQ_{Nf} formation were driven by the $\Delta\tilde{\mu}_{H^+}$-dependent reverse electron flow from ubiquinol to the Complex I redox components. Different sensitivity of the $\Delta\tilde{\mu}_{H^+}$-generating NADH:ubiquinone and $\Delta\tilde{\mu}_{H^+}$-consuming ubiquinol:NAD^+ reductases to the specific inhibitors such as ADP-ribose (Zharova and Vinogradov, 1997), rotenone (Grivennikova *et al.*, 1997), and Triton X-100 (Ushakova *et al.*, 1999) has been interpreted to suggest different electron transfer pathways for either reaction. Much more systematic analysis of the sample reduced by NADH or succinate is evidently needed to check this possibility.

The addition of complex I inhibitors progressively diminished the broadening of the $g_{\|} = 2.05$ signal, resulting in an increase of the $g_{\|} = 2.05$ peak height toward that of the fully reduced uncoupled state. We also observed the same, concomitant changes in the $g_{\|} = 2.05$ signal and in the quenching of the SQ_{Nf} signal by rotenone during the steady state succinate oxidation, where the $\Delta\tilde{\mu}_{H^+}$ formation was maintained by the succinate respiration. Hence, we postulate that the line shape change of the $g_{\|} = 2.05$ signal of cluster N2 is caused by the $\Delta\tilde{\mu}_{H^+}$-sensitive SQ_{Nf} species but not by $\Delta\tilde{\mu}_{H^+}$ itself. These properties are unique to cluster N2 because such changes have not been observed in any other EPR-detectable iron–sulfur clusters to date.

Previously, Burbaev *et al.* proposed the existence of a strong dipole–dipole interaction between SQ_{Nf} and reduced-cluster N2, on the basis of the extremely fast spin relaxation behavior of SQ_{Nf} (Burbaev *et al.*, 1989). The dipole coupling between two spins also leads to a broadening or splitting of the EPR spectrum (Abragam and Bleaney, 1970). On the basis of the splitting of the $g_{||} = 2.05$ peak of cluster N2 with a peak separation of 33 gauss, we estimated the distance between the SQ_{Nf} and cluster N2 to be in the range of 8–11 Å (Vinogradov *et al.*, 1995). Using the equation $\Delta B = \beta \cdot g \cdot r^{-3}\ (1 - 3\cos^2\theta)$, where ΔB is the split peak separation (in magnetic field units), g is the g factor of the SQ_{Nf}, r is the distance between interacting dissimilar spin species, and θ is the angle between

the interdipolar vector and the $g_{||}$ direction of cluster N2 (perpendicular to the membrane plane) (Salerno *et al.*, 1979). We subsequently reported a close correlation between the spin coupling (probed by an increase of the split signal at $g = 2.044$ as well as by the decrease of the nonsplit signal at $g_{||} = 2.05$ of the cluster N2) and the size of the SQ_{Nf} free radical signal in the bovine heart SMP under various redox equilibrium states of complex I in situ (Ohnishi *et al.*, 1998). In contrast, the simulation of the SQ_I broadening (this SQ_I species defined by van Belzen *et al.* apparently corresponds to our SQ_{Nf} species, but the latter is spectrally more strictly resolved) at 16 K has led van Belzen *et al.* to conclude that a broadening of SQ_I signal, which is caused by the interaction with cluster N2, cannot be more than 10 gauss. This is far less than 28 gauss seen by these authors (van Belzen *et al.*, 1997) and 33 gauss by Vinogradov *et al.* (1995) for the $g_{||} = 2.05$ component of cluster N2. Therefore, van Belzen *et al.* concluded that the splitting of the $g_{||} = 2.05$ peak is due to an interaction with another component different from the SQ_I species, possibly the second "cluster N2" residing in the same TYKY (Nqo9/NuoI) subunit. However, both g tensor of N2 and the dipolar interaction are anisotropic, and the dipolar interaction will produce different effects on the SQ_{Nf} signal at each orientation of the magnetic field with respect to the N2 g axes. If we assume that the dipolar interaction tensor is axial and that it has its unique axis along the N2 $g_{||}$ direction, the maximal splitting at $g_{||}$ direction ($\theta = 0$) would be equal to $2g\beta r^{-3}$. Since the g tensor for SQ_{Nf} is isotropic (at X-band no anisotropy is seen), the actual broadening of SQ_{Nf} signal is determined by the averaged splitting. In our case, the averaged splitting will be $0.75g\beta r^{-3}$, which is equal to only $0.75/2 = 0.375$ of the value for N2 $g_{||} = 2.05$ signal split. Therefore, for values of the N2 splitting equal to 28 gauss or 33 gauss, the SQ_{Nf} splitting will be 10 gauss or 12 gauss, respectively, not the value of 28 gauss as van Belzen *et al.* assumed. It would be seen only as the SQ_{Nf} broadening at lower temperatures below 22 K. Thus, the observed splitting of cluster N2 and broadening of SQ_{Nf} signals could be explained by the dipole–dipole interaction between these two redox centers.

To further strengthen our proposal of direct magnetic interaction between SQ_{Nf} and cluster N2, we analyzed enhancement of the $P_{1/2}$ value of SQ_{Nf} species on the basis of the assumption that its enhancement was caused by the iron–sulfur cluster N2. (Detailed calculations are presented in the Appendix.) We have obtained a distance of approximately 11 Å, which is consistent with the distance (8 − 11 Å) calculated based on the splitting of $g_{||} = 2.05$ of cluster N2 (Vinogradov *et al.*, 1995).

Although the molecular mechanism of electron and proton transfer in complex I is still largely unknown, recent biochemical, biophysical, and molecular biological studies have strongly suggested that specific subunits, PSST (Nqo6/NuoB), 49 kDa (Nqo4/NuoD), and ND1 (Nqo8/NuoH) may play important roles in the energy coupling reaction of complex I. Inhibitor induced and/or site-directed mutations indicated 49 kD (Darrouzet and Dupuis, 1997), PSST (Ahlers *et al.*, 2000a; Friedrich, 1998; Kashani-Poor *et al.*, 2001) as well as ND1 subunits (Zickermann *et al.*, 1998) modify the interaction of complex I with quinone and sensitivity toward complex I inhibitors. Using a highly tritiated photoaffinity-labelled pyridaben analogue as a probe, a tight inhibitor-binding site was shown in PSST and a low affinity site in ND1 subunits (Schuler *et al.*, 1999), and possible functional coupling between these two subunits was also suggested (Schuler *et al.*, 1999; Schuler and Casida, 2001).

In addition, cluster N2 was indicated to be coordinated by three cysteines from PSST (Ahlers *et al.*, 2000a; Friedrich, 1998) and likely by one noncysteine ligand from 49 kDa subunit (Kashani-Poor *et al.*, 2001). Evolutionary process of the functional core originated from the anaerobic [NiFe] hydrogenase to that in the aerobic complex I predicted the birth of a unique functional core of complex I containing cluster N2 and the $\Delta\tilde{\mu}_{H^+}$-sensitive SQ_{Nf} (Friedrich and Scheide, 2000; Kerscher *et al.*, 2001; Yano and Ohnishi, 2001). The proton translocation through the membrane part of complex I most likely operates in the transmembrane subunits ND1 (Nqo8/NuoH) and ND2/ND4/ND5 (Nqo14/NuoN)/(Nqo13/NuoM)/(Nqo12/NuoL), which are also conserved among membrane bound [NiFe] hydrogenases (Albracht, 1993; Friedrich and Scheide, 2000; Friedrich and Weiss, 1997). The latter three subunits appear to have evolved from a common ancestor, sharing their roots with Na^+/H^+ or K^+/H^+ transporters (Friedrich and Scheide, 2000; Friedrich and Weiss, 1997; Hamamoto *et al.*, 1994).

In this connection, the following recent experimental observations are very interesting: (1) Sazanov *et al.* have resolved the membrane part of complex I into two parts (Sazanov *et al.*, 2000), and they suggested that ND4/ND5 and ND1/ND2 transmembrane subunit pairs may form two major domains of the membrane part. (2) Fisher and Rich (2000) recognized a triad sequence motif(s) as the Q-binding site(s) in some quinone oxidoreductases. Utilizing this motif(s), they predicted that two transmembrane subunits of complex I, namely ND4 (Nqo13/NuoM) and ND5 (Nqo12/NuoL) may harbor a Q_i-type and a Q_A-type Q-binding site motifs, respectively. A more general triad of Q-binding motif was also found in the highly conserved

N-terminal region of the 49 kDa subunit (Dupuis *et al.*, 2001). (3) Steuber *et al.* reported that Na^+ is primarily transported, coupled with electron transport in some enterobacterial complex I (Steuber, 2001; Steuber *et al.*, 2000). These observations suggest a possibility that energy transducing reactions in complex I with total stoichiometry $H^+/2e^-$ of 4 are operated by two different mechanisms.

In the present work, we have shown the presence of three distinct SQ species showing strikingly different spin relaxation properties, which implies their different spatial location relative to the cluster N2. However, to elucidate the energy coupling mechanism in complex I, further studies on the effect of other complex I inhibitors (Degli Esposti, 1998; Friedrich *et al.*, 1994; Miyoshi, 1998; Okun *et al.*, 1999) on the cluster N2 and three SQ species, SQ_{Nf}, SQ_{Ns}, and SQ_{Nx}, characterization of thermodynamic properties of individual SQ species, and on the membrane spatial location of these components are required. Such attempts are currently being made in our laboratories.

APPENDIX: CALCULATION OF THE DISTANCE BETWEEN THE IRON–SULFUR CLUSTER N2 AND THE FAST-RELAXING UBISEMIQUINONE, BASED ON THE SPIN RELAXATION ENHANCEMENT OF THE LATTER COMPONENT BY THE FORMER

According to Rupp *et al.* (Rupp *et al.*, 1978), absolute value of magnetic field H_1 is related to microwave power P as follows:

$$H_1^2 = K \cdot P \tag{1}$$

For the magnetic field ($H_{1/2}$) corresponding to the value of half-saturation ($P_{1/2}$), the next equation is valid (Poole, 1967):

$$\frac{1}{4} H_{1/2}^2 \gamma^2 T_1 T_2 = 1 \tag{2}$$

From the Eqs. (1) and (2), the following is derived:

$$P_{1/2} = K' \cdot \frac{4}{\gamma^2 T_1 T_2} \tag{3}$$

Where T_1 is the spin–lattice relaxation time, T_2 is spin–spin relaxation time, γ is gyromagnetic ratio, K and K' are constants ($K' \sim K \sim 1$) (Poole, 1967). We assume that two interacting paramagnetic centers with a "slow"- and a "fast"-relaxing spins are fixed in a matrix and that the distance (r) between centers does not change. Since the interaction between two centers affects the relaxation properties of the slow-relaxing spin, the relaxation times T_1 and T_2 can be given as follows:

$$\frac{1}{T_1} = \left(\frac{1}{T_1}\right)_{\text{in}} + \left(\frac{1}{T_1}\right)_{d} + \left(\frac{1}{T_1}\right)_{\text{ex}} \tag{4}$$

$$\frac{1}{T_2} = \left(\frac{1}{T_2}\right)_{\text{in}} + \left(\frac{1}{T_2}\right)_{d} + \left(\frac{1}{T_2}\right)_{\text{ex}} \tag{5}$$

Where subscript in denotes intrinsic (magnetically isolated SQ) spin–lattice or spin–spin relaxation times of the slow-relaxation paramagnetic center, d is the contribution to the relaxation time from the dipole–dipole interaction between the two centers, ex is the contribution from the scalar exchange coupling between interacting spins. The most probable interaction partner for the SQ_{Nf} is iron–sulfur cluster N2 (Ohnishi, 1998; Ohnishi *et al.*, 1998; Vinogradov *et al.*, 1995). The Eqs. (4) and (5) can be simplified if the intrinsic (without interaction) spin–lattice relaxation time of ubisemiquinone is much longer than that of spin–lattice relaxation in the presence of interaction. Then we can ignore the first term in the Eq. (4). According to (Abragam and Bleaney, 1970; Goodman and Leigh, 1985; Hirsh *et al.*, 1992; Kulikov *et al.*, 1972), the dipole contribution can be expressed as follows:

$$\left(\frac{1}{T_1}\right)_d = \frac{\gamma_0^2 \mu^2}{r^6}\left(\frac{1}{6}B + 3C + \frac{3}{2}E\right) \tag{6}$$

$$\left(\frac{1}{T_2}\right)_d = \frac{\gamma_0^2 \mu^2}{r^6}\left(\frac{1}{3}A + \frac{1}{12}B + \frac{3}{2}C + 3D + \frac{3}{4}E\right) \tag{7}$$

The terms A–E are defined as follows:

$$A = \tau_1(1 - 3\ \cos^2\Theta)^2$$

$$B = \frac{\tau_2}{1 + (\omega_0 - \omega)^2\tau_2^2}(1 - 3\ \cos^2\Theta)^2$$

$$C = \frac{\tau_1}{1 + \omega_0^2\tau_1^2}\ \sin^2\Theta \cdot \cos^2\Theta$$

$$D = \frac{\tau_2}{1 + \omega^2\tau_2^2}\ \sin^2\Theta \cdot \cos^2\Theta$$

$$E = \frac{\tau_2}{1 + (\omega_0 + \omega)^2\tau_2^2}\ \sin^4\Theta$$

Where τ_1 and τ_2 are spin–lattice and spin–spin relaxation times of the fast-relaxing transition metal center (iron–sulfur cluster N2), γ_0 is the gyromagnetic ratio for the slow-relaxing radical spin (SQ_{Nf}), the μ is the magnetic moment of the fast-relaxing spin, ω_0 and ω are resonance frequencies for the slow- and fast-relaxing centers, and Θ is the angle between the magnetic field direction and the interspin vector. The Eqs. (6) and (7) are valid within the Redfield limit (Redfield, 1955) where τ_1 must be smaller than T_1 and also $\tau_2 < T_2$ (Goodman and Leigh, 1985;

Hirsh *et al.*, 1992). These requirements are met in our system. For an approximate estimation of the distance (r) between the two paramagnetic centers, we can consider only dipole–dipole interaction first and then include the exchange term.

The Eqs. (6) and (7) contain τ_1 and τ_2 for the fast-relaxation center, cluster N2. At 40 K the N2 signal becomes completely broadened because of its rapid spin–lattice relaxation (τ_1 is extremely short). Since $\tau_2 \leq \tau_1$, we used an approximation as that $\tau_2 = \tau_1$. According to Burbaev *et al.* (1983), τ_1 of the N2 is given as follows within the temperature range of our measurement:

$$\frac{1}{\tau_1} = 2.4 \times 10^{10} \exp\left(-\frac{145}{T}\right) \tag{8}$$

Where T is a sample temperature. For ω_0 in the Eqs. (6) and (7) we can use the equation $\omega_0 = 2\pi\nu_0$ where ν_0 is a work frequency of spectrometer, 9.45×10^9 Hz. The ω can be obtained from the equation $\frac{\omega_0}{g_0} = \frac{\omega}{g}$ and then $\omega = \frac{g}{g_0}\omega_0$ (Burbaev and Voevodskaya, 1985; Hirsh *et al.*, 1992). From the Eq. (8), $\tau_1 = 1.56 \times 10^{-9} \cong 1.6 \times 10^{-9}$ s can be obtained at 40 K. According to Chumakov *et al.* (1966), T_2 value is $>10^{-7}$ s for ubisemiquinones. For our estimations we define $T_2 = 2 \times 10^{-7}$ s. Using the values of g_0 and ω_0 for the SQ_{Nf} and g, τ_1, τ_2, and ω for cluster N2, we can determine the distance. For the dipole–dipole interaction, the half-saturation power is:

$$P_{1/2} = \frac{4}{\gamma_0^2}\left(\frac{1}{T_1}\right)\left(\frac{1}{T_2}\right) = \frac{4}{\gamma_0^2}\left(\frac{1}{T_1}\right)_d\left[\left(\frac{1}{T_2}\right)_d + \left(\frac{1}{T_2}\right)_{\text{in}}\right] \tag{9}$$

Substitution of $(1/T_1)_d$ and $(1/T_2)_d$ in (9) with the first main terms of Eqs. (6) and (7) gives:

$$P_{1/2} = \frac{4}{\gamma_0^2}\frac{\mu^2\gamma_0^2}{r^6}\frac{1}{6}\frac{\tau_2}{1+\left(\omega_0 - \frac{g}{g_0}\omega_0\right)^2\tau_2^2}(1 - 3\cos^2\Theta)^2 \times\left[\frac{\gamma_0^2\mu^2}{r^6}\frac{1}{3}\tau_1(1-3\cos^2\Theta)^2 + \left(\frac{1}{T_2}\right)_{\text{in}}\right] \tag{10}$$

And then

$$P_{1/2} = \frac{2}{3}\frac{\mu^2}{r^6}\frac{\tau_2}{1+\left(1-\frac{g(\Theta')}{g_0}\right)^2\omega_0^2\tau_2^2}(1-3\cos^2\Theta)^2 \times\left[\frac{\gamma_0^2\mu^2\tau_1}{3r^6}(1-3\cos^2\Theta)^2 + \left(\frac{1}{T_2}\right)_{\text{in}}\right] \tag{11}$$

Where Θ' is the angle between Z axis of the N2 g tensor and the magnetic field direction. After averaged over angles, the following equation can finally be obtained:

$$P_{1/2} = \frac{8}{15}\frac{\gamma^2\hbar^2 S(S+1)}{r^6}\frac{\tau^2}{1+\left(1-\frac{g_{\text{av}}}{g_0}\right)^2\omega_0^2\tau_2^2} \times\left[\frac{4\gamma_0^2\gamma^2\hbar^2 S(S+1)\tau_1}{15r^6} + \left(\frac{1}{T_2}\right)_{\text{in}}\right] \tag{12}$$

Here we have used the following equations: $\mu^2 = g^2\beta^2 S(S+1) = \gamma^2\hbar^2 S(S+1)$ because $\gamma = \frac{g\beta}{\hbar}$ where β is the Bohr magneton and $\hbar = h/2\pi$, which is the Planck constant. If $g_{\text{av}} = 1.966$ (for N2), $P_{1/2} = 220$ mW, $g_0 = 2.004$, $S = {}^1/_2$, $\tau_1 = \tau_2 = 1.6 \times 10^{-9}$ s, $\omega_0 = 5.937 \times 10^{10}$, $(T_2)_{\text{in}} = 2 \times 10^{-7}$ s, then we obtained the estimated distance $r = 12$ Å. According to Brudvig *et al.* (1984), we should take $g = 1.93$ as the most probable g value for cluster N2, which accords with the maximum of absorption. With $g = 1.93$, we obtained the estimated distance $r = 11$ Å.

We estimated the distance (r), assuming that the exchange term in the Eqs. (4) and (5) was much smaller than the dipole term. Now we can evaluate how an inclusion of the exchange term affects the distance estimation. The contribution of the exchange to the relaxation time can be expressed as follows according to Abragam and Bleaney (1970) and Hirsh *et al.* (1992):

$$\left(\frac{1}{T_1}\right)_{\text{ex}} = \frac{2}{3}(J_{\text{ex}})^2 S(S+1)\frac{\tau_2}{1+(\omega_0-\omega)^2\tau_2^2} \tag{13}$$

$$\left(\frac{1}{T_2}\right)_{\text{ex}} = (J_{\text{ex}})^2\frac{S(S+1)}{3}\left(\frac{\tau_2}{1+(\omega_0-\omega)^2\tau_2^2} + \tau_1\right) \tag{14}$$

The last parts of Eqs. (13) and (14) are angle-independent terms of A and B in Eq. (7). J_{ex} is the scalar exchange coupling constant, and S is the quantum spin number of the fast-relaxing spin. According to Goodman and Leigh (1985), the scalar exchange coupling constant J_{ex} is 3×10^{-4} cm^{-1} $= 9 \times 10^6$ Hz for the distance range $r = 8$–13 Å. Thus, calculation of the exchange term gives the value $(\frac{1}{T_1})_{\text{ex}} = 1.5 \times 10^4$ s^{-1}. For this distance range the $(\frac{1}{T_1})_d$ calculated from the Eq. (6) gives the value $>10^6$ s^{-1}. These two terms are more than two orders of magnitude smaller:

$$\left(\frac{1}{T_1}\right)_{\text{ex}} \ll \left(\frac{1}{T_1}\right)_d \text{ similarly } \left(\frac{1}{T_2}\right)_{\text{ex}} \ll \left(\frac{1}{T_2}\right)_d$$

Thus, the inclusion of the exchange term to the calculation only affects the final answer by hundredths digit (cf. Rabenstein and Shin, 1995). The distance calculated from the splitting constant of the $g_{||}$ component of iron–sulfur cluster N2 and that from the relaxation enhancement of the SQ_{Nf} signal due to interaction with N2 (this work)

gave the consistent values of 8–11 Å (Vinogradov *et al.*, 1995).

ACKNOWLEDGMENTS

This work was supported by National Institute of Health Grant No. R01GM30736 to T. Ohnishi and NIH Fogarty International Research Collaborative Grant No. RO3TW00140–01A2 to T. Ohnishi and A. Vinogradov. V. G. Grivennikova and A. D. Vinogradov were partially supported by Russian Foundation for Fundamental Research Grant No. 99-04-48082. We are indebted to Drs John C. Salerno and Russell LoBrutto for their stimulating and helpful discussion. The authors are also grateful to Dr S. Tsuyoshi Ohnishi for inventing a special rapid mixing device to add and mix a small amount of chemicals to the sample in an EPR tube, and to Mr Robert Lin for his excellent technical assistance. We also express our gratitude to Dr W. R. Widger in the Department of Biology and Biochemistry, University of Houston, Houston, Texas, and Dr T. Friedrich in the Institute for Organic Chemistry and Biochemistry, Albert-Ludwigs-University, Freiburg, Germany, for their generous gifts of piericidin A.

REFERENCES

Aasa, R., and Vänngård, T. (1975). *J. Magn. Res.* **19**, 308–315.
Abragam, A., and Bleaney, B. (1970). *Electron Paramagnetic Resonance of Transition Ions*, Calendar Press, Oxford.
Ahlers, P. M., Garofano, A., Kerscher, S. J., and Brandt, U. (2000a). *Biochim. Biophys. Acta* **1459**, 258–265.
Ahlers, P. M., Zwicker, K., Kerscher, S., and Brandt, U. (2000b). *J. Biol. Chem.* **275**, 23577–23582.
Albracht, S. P. (1993). *Biochim. Biophys. Acta* **1144**, 221–224.
Beinert, H., and Albracht, S. P. (1982). *Biochim. Biophys. Acta* **683**, 245–277.
Bowyer, J. R., and Ohnishi, T. (1985). EPR spectroscopy in the study of ubisemiquinones in redox chains. In *Coenzyme Q* (Lenaz, G., ed.), Wiley, New York, pp. 409–432.
Brandt, U. (1997). *Biochim. Biophys. Acta* **1318**, 79–91.
Brandt, U. (1999). *Biofactors* **9**, 95–101.
Brown, G. C., and Brand, M. D. (1988). *Biochem. J.* **252**, 473–479.
Brudvig, G. W., Blair, D. F., and Chan, S. I. (1984). *J. Biol. Chem.* **259**, 11001–11009.
Burbaev, D. S., Blumenfeld, L. A., and Zviagilskay, R. A. (1983). *Biofizika* **28**, 292–297.
Burbaev, D. S., Moroz, I. A., Kotlyar, A. B., Sled, V. D., and Vinogradov, A. D. (1989). *FEBS Lett.* **254**, 47–51.
Burbaev, D. S., and Voevodskaya, N. V. (1985). *Zurnal Fizicheskoi Khimii* **59**, 2287–2291.
Cammack, R., Williams, R., Guigliarelli, B., More, C., and Bertrand, P. (1994). *Biochem. Soc. Trans.* **22**, 721–725.
Chumakov, V. M., Kalinichenko, L. P., and Kalmanson, A. E. (1966). *Biofizika* **11**, 910–913.
Darrouzet, E., and Dupuis, A. (1997). *Biochim. Biophys. Acta* **1319**, 1–4.
Degli Esposti, M. (1998). *Biochim. Biophys. Acta* **1364**, 222–235.
Degli Esposti, M., and Ghelli, A. (1994). *Biochim. Biophys. Acta* **1187**, 116–120.
de Jong, A. M. P., and Albracht, S. P. J. (1994). *Eur. J. Biochem.* **222**, 975–982.
de Jong, A. M., Kotlyar, A. B., and Albracht, S. P. (1994). *Biochim. Biophys. Acta* **1186**, 163–171.
Di Virgilio, F., and Azzone, G. F. (1982). *J. Biol. Chem.* **257**, 4106–4113.
Dupuis, A., Prieur, I., and Lunardi, J. (2001). *J. Bioenerg. Biomembr.* **33**, 159–168.
Dutton, P. L., Moser, C. C., Sled, V. D., Daldal, F., and Ohnishi, T. (1998). *Biochim. Biophys. Acta* **1364**, 245–257.
Faeder, E. J., and Siegel, L. M. (1973). *Anal. Biochem.* **53**, 332–336.
Finel, M., Majander, A. S., Tyynelä, J., De Jong, A. M. P., Albracht, S. P. J., and Wikström, M. (1994). *Eur. J. Biochem.* **226**, 237–242.
Fisher, N., and Rich, P. R. (2000). *J. Mol. Biol.* **296**, 1153–1162.
Friedrich, T. (1998). *Biochim. Biophys. Acta* **1364**, 134–146.
Friedrich, T., and Scheide, D. (2000). *FEBS Lett.* **479**, 1–5.
Friedrich, T., van Heek, P., Leif, H., Ohnishi, T., Forche, E., Kunze, B., Jansen, R., Trowitzsch-Kienast, W., Höfle, G., Reichenbach, H., and Weiss, H. (1994). *Eur. J. Biochem.* **219**, 691–698.
Friedrich, T., and Weiss, H. (1997). *J. Theor. Biol.* **187**, 529–540.
Galkin, A. S., Grivennikova, V. G., and Vinogradov, A. D. (1999). *FEBS Lett.* **451**, 157–161.
Goodman, G., and Leigh, J. S., Jr. (1985). *Biochemistry* **24**, 2310–2317.
Gornall, A. B., Bardwill, C. S., and David, M. M. (1949). *J. Biol. Chem.* **177**, 751–766.
Grivennikova, V. G., Maklashina, E. O., Gavrikova, E. V., and Vinogradov, A. D. (1997). *Biochim. Biophys. Acta* **1319**, 223–232.
Hamamoto, T., Hashimoto, M., Hino, M., Kitada, M., Seto, Y., Kudo, T., and Horikoshi, K. (1994). *Mol. Microbiol.* **14**, 939–946.
Hatefi, Y. (1985). *Annu. Rev. Biochem.* **54**, 1015–1069.
Hirsh, D. J., Beck, W. F., Lynch, J. B., Que, L., Jr., and Brudvig, G. W. (1992). *J. Am. Chem. Soc.* **114**, 7475–7481.
Ingledew, W. J., and Ohnishi, T. (1980). *Biochem. J.* **186**, 111–117.
Kashani-Poor, N., Zwicker, K., Kerscher, S., and Brandt, U. (2001). *J. Biol. Chem.* **276**, 24082–24087.
Kerscher, S., Kashani-Poor, N., Zwicker, K., Zickermann, V., and Brandt, U. (2001). *J. Bioenerg. Biomembr.* **33**, 187–196.
Kotlyar, A. B., Sled, V. D., Burbaev, D. S., Moroz, I. A., and Vinogradov, A. D. (1990). *FEBS Lett.* **264**, 17–20.
Kotlyar, A. B., Sled, V. D., and Vinogradov, A. D. (1992). *Biochim. Biophys. Acta* **1098**, 144–150.
Kotlyar, A. B., and Vinogradov, A. D. (1990). *Biochim. Biophys. Acta* **1019**, 151–158.
Krishnamoorthy, G., and Hinkle, P. C. (1988). *J. Biol. Chem.* **263**, 17566–17575.
Kulikov, A. V., Likhtenshtein, G. I., Rozantsev, E. G., Suskina, V. I., and Shapiro, A. B. (1972). *Biofizika* **17**, 42–48.
Lee, C.-P., and Ernster, L. (1967). *Methods Enzymol.* **10**, 543–548.
Leif, H., Sled, V. D., Ohnishi, T., Weiss, H., and Friedrich, T. (1995). *Eur. J. Biochem.* **230**, 538–548.
Leigh, J. S. J. (1970). *J. Chem. Phys.* **52**, 2608–2612.
Lenaz, G. (1998). *Biochim. Biophys. Acta* **1364**, 207–221.
Meinhardt, S. W., Kula, T., Yagi, T., Lillich, T., and Ohnishi, T. (1987). *J. Biol. Chem.* **262**, 9147–9153.
Miki, T., Yu, L., and Yu, C. A. (1992). *Arch. Biochem. Biophys.* **293**, 61–66.
Mitchell, P. (1966). *Biol. Rev. Camb. Philos. Soc.* **41**, 445–502.
Miyoshi, H. (1998). *Biochim. Biophys. Acta* **1364**, 236–244.
Ohnishi, T. (1979). Mitochondrial iron–sulfur flavodehydrogenases. In *Membrane Proteins in Energy Transduction* (Capaldi, R. A., ed.), Marcel Dekker, New York, pp. 1–87.
Ohnishi, T. (1998). *Biochim. Biophys. Acta* **1364**, 186–206.
Ohnishi, T., and Salerno, J. C. (1982). Iron–sulfur clusters in the mitochondrial electron-transport chain. In *Iron–Sulfur Proteins, Vol. 4* (Spiro, T. G., ed.), Wiley, New York, pp. 285–327.
Ohnishi, T., Sled, V. D., Yano, T., Yagi, T., Burbaev, D. S., and Vinogradov, A. D. (1998). *Biochim. Biophys. Acta* **1365**, 301–308.
Okun, J. G., Lummen, P., and Brandt, U. (1999). *J. Biol. Chem.* **274**, 2625–2630.

Poole, C. P. J. (1967). *Electron Spin Resonance. A Comprehensive Treatise on Experimental Techniques*, Interscience, New York.
Rabenstein, M. D., and Shin, Y. K. (1995). *Proc. Natl. Acad. Sci. U.S.A.* **92**, 8239–8243.
Ragan, C. I. (1990). *Biochem. Soc. Trans.* **18**, 515–516.
Rasmussen, T., Scheide, D., Brors, B., Kintscher, L., Weiss, H., and Friedrich, T. (2001). *Biochemistry* **40**, 6124–6131.
Redfield, A. G. (1955). *Phys. Rev.* **98**, 1787–1809.
Rieske, J. S. (1967). *Methods Enzymol.* **10**, 488–493.
Rupp, H., Rao, K. K., Hall, D. O., and Cammack, R. (1978). *Biochim. Biophys. Acta* **537**, 255–260.
Salerno, J. C., Blum, H., and Ohnishi, T. (1979). *Biochim. Biophys. Acta* **547**, 270–281.
Sazanov, L. A., Peak-Chew, S. Y., Fearnley, I. M., and Walker, J. E. (2000). *Biochemistry* **39**, 7229–7235.
Scholes, T. A., and Hinkle, P. C. (1984). *Biochemistry* **23**, 3341–3345.
Schuler, F., and Casida, J. E. (2001). *Biochim. Biophys. Acta* **1506**, 79–87.
Schuler, F., Yano, T., Di Bernardo, S., Yagi, T., Yankovskaya, V., Singer, P. T., and Casida, J. E. (1999). *Proc. Natl. Acad. Sci. U.S.A.* **96**, 4149–4153.
Steuber, J. (2001). *J. Bioenerg. Biomembr.* **33**, 179–186.
Steuber, J., Schmid, C., Rufibach, M., and Dimroth, P. (2000). *Mol. Microbiol.* **35**, 428–434.
Ushakova, A. V., Grivennikova, V. G., Ohnishi, T., and Vinogradov, A. D. (1999). *Biochim. Biophys. Acta* **1409**, 143–153.
van Belzen, R., Kotlyar, A. B., Moon, N., Dunham, W. R., and Albracht, S. P. J. (1997). *Biochemistry* **36**, 886–893.
Vinogradov, A. D. (1993). *J. Bioenerg. Biomembr.* **25**, 367–375.
Vinogradov, A. D., Sled, V. D., Burbaev, D. S., Grivennikova, V. G., Moroz, I. A., and Ohnishi, T. (1995). *FEBS Lett.* **370**, 83–87.
Walker, J. E. (1992). *Q. Rev. Biophys.* **25**, 253–324.
Wang, D.-C., Meinhardt, S. W., Sackmann, U., Weiss, H., and Ohnishi, T. (1991). *Eur. J. Biochem.* **197**, 257–264.
Weiss, H., and Friedrich, T. (1991). *J. Bioenerg. Biomembr.* **23**, 743–754.
Weiss, H., Friedrich, T., Hofhaus, G., and Preis, D. (1991). *Eur. J. Biochem.* **197**, 563–576.
Wikström, M. (1984). *FEBS Lett.* **169**, 300–304.
Yano, T., Magnitsky, S., Sled, V. D., Ohnishi, T., and Yagi, T. (1999). *J. Biol. Chem.* **274**, 28598–28605.
Yano, T., and Ohnishi, T. (2001). *J. Bioenerg. Biomembr.* **33**, 213–222.
Yano, T., and Yagi, T. (1999). *J. Biol. Chem.* **274**, 28606–28611.
Zharova, T. V., and Vinogradov, A. D. (1997). *Biochim. Biophys. Acta* **1320**, 256–264.
Zickermann, V., Barquera, B., Wikström, M., and Finel, M. (1998). *Biochemistry* **37**, 11792–11796.